View metadata, citation and similar papers at core.ac.uk
brought to you by CORE
provided by Ghent University Academic Bibliography

Guidelines for participatory noise sensing based on analysis of high quality mobile noise measurements

Luc Dekoninck[a)]
Dick Botteldooren[b)]
Information Technology, Acoustics Group, Ghent University
St-Pietersnieuwstraat 41, 9000 Ghent, Belgium[a,b]

Luc Int Panis[c,d)]
Flemish Institute for Technological Research (VITO), Boeretang 200, 2400 Mol, Belgium[c]
Transportation Research Institute (IMOB), Hasselt University, Wetenschapspark 5 bus 6, 3590 Diepenbeek, Belgium[d]

Measuring noise and air pollution by participatory sensing is becoming a popular approach to gather traffic related pollution data. Both exposures are related to the traffic intensity and traffic dynamics on the travelled road. Mobile noise measurements are cheaper and easier to perform than mobile air pollution measurements and they are a promising proxy to predict personal air pollution exposure. In this paper, the theoretical relation between noise and air pollution is compared with more than 100 hours of combined mobile noise and black carbon measurements. The relation between spectral content, traffic dynamics and black carbon exposure provides relevant parameters to predict local air pollution exposure. Low frequency noise – related to engine noise – correlates better with both the theoretical air pollution emission and the mobile Black Carbon measurements. The difference between high and low frequency spectral content relates to the speed of the traffic flow. Time sampling below a one second resolution is relevant to detect attributes of the traffic dynamics. Based on these observations, guidelines and requirements for mobile-phone-based noise measurements in participatory sensing projects are compiled.

[a)] email: luc.dekoninck@intec.ugent.be
[b)] email: dick.botteldooren@intec.ugent.be
[c)] email: luc.intpanis@vito.be; luc.intpanis@uhasselt.be

1 INTRODUCTION

Mobile noise measurements are a popular theme in noise exposure modeling. (Eisenman et al., 2009; Kanjo et al., 2010, Maissonneuve et al., 2009). They can be useful to enhance noise mapping and noise exposure modeling by adding more detailed emission parameters related to the traffic dynamic which are currently only rarely included in the noise mapping procedures. Mobile noise measurements can be done with low intrusive measurement equipment like dosimeters and the new mobile technologies. Noise is also strongly related to the traffic related air pollution exposure and might be a good proxy to model personal air pollution exposure (Can et al, 2011; Can et al, 2011b; De Coensel et al. 2007; Eisenman et al. 2009, Foraster et al., 2011).

An experiment was set up measuring both the noise and black carbon exposure on a bicycle for one year, travelling many different roads in actual commuting condition (during rush hour). From this experiment the noise measurements are used to predict the black carbon exposure. In this paper we focus on the noise properties that proved to be relevant in the modeling of BC. These findings are compiled in a set of guidelines and recommendations for future projects assessing mobile noise exposure measurements. If the guidelines are fulfilled the potential to use the mobile noise measurements as a proxy for air pollution related exposure will dramatically improve.

First we will address the theoretical aspects of both noise emission and air pollution in relation to the traffic dynamics, identifying the potential correlations between the spectral content of the mobile noise measurements and the vehicle exhaust dynamics. In a second section we will address the properties of the mobile noise measurements and present the spatial evaluations. In a third section we will present the noise parameters with the best correlation to the black carbon and discuss the effect of the sparse sampling and its stability for both noise and black carbon. Finally a set of guidelines are compiled to perform future mobile noise measurements.

2 THEORETICAL ASPECTS OF TRAFFIC NOISE AND AIR POLLUTION

Both noise level and the local component of air pollution can be attributed to traffic. By investigating theoretical emission of noise and air pollutants in typical traffic flows, noise indicators that can be used as proxies for air pollution can be identified. For this purpose, the noise emission was modeled according the Harmonoise model (Salomons et al, 2011) and the air pollution was modeled according to the Versit+ emission model (Smit et al., 2007). A realistic set of speed and acceleration data is retrieved from a traffic micro-simulation model in major city in Flanders. For each combination of speed and acceleration the corresponding one-third octave band noise emission spectrum and the air pollution emission (CO_2, NO_x and PM_{10}) was calculated for a standard vehicle (person car type). The one-third octave bands were aggregated in four groups, each presenting a typical part of the spectrum. Base frequencies, $L_{OBFeq,1s}$, is defined as the energetic sum of bands 25 to 80 Hz, low frequency, $L_{OLFeq,1s}$ sums bands 100 to 200 Hz, mid frequency, $L_{OMFeq,1s}$ bands 400 and 500 Hz, and finally high frequency, $L_{OHFeq,1s}$, bands 1000 to 2000 Hz. In Table 1, the cross correlation between air pollutant emission per second of the vehicle stream and the noise indicators defined above, is given for the urban driving test situation. The air pollution parameters are log10 converted to match the noise evaluation.

The correlation between the low frequency noise indicators $L_{BLFeq,1s}$ and $L_{OLFeq,1s}$ and the air pollution emissions is in general higher than the correlation between L_{Aeq} and these emissions.

This is not unexpected. The Harmonoise emission model relates high frequency noise emissions mainly to rolling noise and low frequency noise emission mainly to engine and drive train noise. In addition, acceleration increases engine power and thus also increases the low frequency contribution. The A-weighted total noise emission is clearly determined by the higher frequencies, corresponding with the rolling noise and as such a less useful indicator for air pollutant emission. It nevertheless increases linearly with the number of vehicles as does the overall air pollutant emission. .CO_2 emission is directly related to the power produced by the engine and thus is expected to be somewhat correlated to high frequency components since they indicate high driving speed. The difference $L_{HFmLF,1s}$ between high and low frequencies is thought to be more exclusively related to rolling noise and thus correlates poorly with CO_2 emission. For particulate matter emission (PM_{10}), the correlation of the noise parameters decreases quite strongly from $L_{BLFeq,1s}$ to $L_{OLFeq,1s}$, $L_{OMFeq,1s}$, L_{Aeq} and $L_{OHFeq,1s}$. The relationship of PM_{10} emission with engine power is more difficult since PM_{10} is a product of incomplete combustion and thus peaks during accelerating and decelerating. Accelerating increases (low-frequency) noise but decelerating does not, yet after a deceleration phase, an acceleration phase is expected.

3 MEASUREMENT SETUP

3.1 Measurement equipment and setup

Measurements of noise and air pollution (Black Carbon) are performed while commuting by bicycle. The experimental setup contains a basic GPS (in a HTC Desire smart phone), a Type 1 Noise Level Meter (Svantek 959) and a micro-aethalometer (Model AE51 MageeScientific, 2009) to measure Black Carbon. The measurement equipment was mounted in a bicycle bag and attached to the steering wheel. The GPS device was put on top of the bag to get the best possible gps readings. The noise equipment is calibrated on regular intervals using a Svantek SV30A Acoustic calibrator. One-third octave band spectra are measured with a time interval of 1/10 second. The very short time interval was chosen for different reasons.

- Biking in itself is noisy so the effect on the noise measurement has to be evaluated. The impact of the type and quality of road surface on the noise measurements was evaluated but was not significant.
- Ashort measurement also allows detecting single car passage noise events. At a time resolution of one second it would be impossible to separate and count the consecutive vehicle passages.

3.2 Location and measurement period

The measurements were performed while commuting by bicycle in suburban and urban areas in Ghent, Flanders (The third city of Belgium with a population of 250.000 and population density is 1500 people per km^2). Ghent is located at the intersection of two important highways, has a major port and industrial area.. The medieval inner city mainly has three storey buildings. It is surrounded by suburbs and villages where a mixture of detached houses and street canyons of two floor buildings can be found. High rise buildings are relatively rare. The commuting trips are performed from the villages to the west of the city into the city center, covering the sparse build areas in the villages, the city center, and open recreational areas and natural reserves in between. The majority of the measurements are performed during the morning and evening rush hour over a period of 12 months, not including public holidays (December 2010 to November

2011). Since all measurements are conducted in rush hour conditions during normal working days, the typical traffic situation is in first order constant for each observation at a given location.

The geographic scope of the trips was extended to measure a diverse mixture of traffic types (pedestrian zone, bus routes etc…), spatial layout (highways, street canyons, local ring roads, medieval city center, etc.) and special biking facilities (dedicated cycle paths, underpasses,…). A total of 209 biking trips were performed, covering a distance of 2300 kilometer, a total measurement time of 128 hours at an average speed of 18 km per hour. Over 75 km of roads were sampled at least 3 times.

3.3 Data cleaning and aggregation

Cleaning of the GPS and Black Carbon (BC) data will not be addressed in detail since this is not the main topic of this article. The contribution of local traffic to the measured BC concentration is of main interest so the background level measured by an official measurement station in the neighborhood is subtracted from the measurement. The local contribution BC_{loc} for a location *i* and a time *j*, can be written as:

$$BC_{loc,i,j} = BC_{i,j} - BC_{j,background}$$

The noise measurements are preprocessed to a one second resolution at the one hand by calculating the one-second equivalent level, $L_{Aeq,1s}$, at the other hand by selecting the lowest 100 ms, $L_{Amin,1s}$. In addition, the frequency band sums defined in Section 2 are calculated.

The measurements are mapped to the traffic network by using aggregation points, p_x, along the network with an interspatial distance of 50 m. The gps-locations are matched to the nearest aggregation point on the network, including restrictions on driving direction and bicycles' accessibility. For each specific passage, $trip_j$, at a specific aggregation point the arithmetic average of all one second measurements is calculated and this for all indicators defined above. For example for L_{Aeq}.

$$L_{Aeq,trip_j,p_x} = \frac{1}{n}\sum_{i=1}^{n} L_{Aeq,1s}\left(t_i, trip_j, p_x\right)$$

with *n* the number of samples for *trip j* at p_x and $L_{Aeq,1s}\left(t_i, trip_j, p_x\right)$ the samples for *trip j* at p_x. Note that the number of samples will be influenced by the cycling speed during a trip at a location. At the typical speed of 18 km/h the distance of 50 m between the aggregation points is covered in 10 seconds so *n* will be 10. Finally the arithmetic average (Avg), standard deviation (sd), and error on the mean (sderror) over the different trips is calculated for all parameters.

4. ANALYSIS OF SPARSE NOISE MEASUREMENTS

4.1 Spatial variation of noise parameters

Figure 1 presents $Avg(L_{Aeq})_{p_x}$ and $Avg(L_{OLF})_{p_x}$ for the aggregation points with at least three bicycle passages. The engine related noise $Avg(L_{OLF})_{p_x}$ is potentially and important indicator for predicting air pollution as derived in Section 2. In both figures, high density roads are clearly visible.

It is important to notice the spatial smoothness of $\mathrm{Avg}(L_{\mathrm{OLF}})_{\mathrm{p_x}}$ compared to $Avg(L_{Aeq})_{p_x}$. Thus in addition to potentially being a better indicator for air pollution, the low frequency component of the noise also seems less sensitive to errors introduced by the sparse sampling probably because of lower sensitivity to disturbing sounds. Important in this spatial evaluation is the emergence of the dynamic traffic conditions in the vicinity of traffic lights where vehicles accelerate. The local noise propagation situation is also influencing the results, for example near the highway bank and noise screen. Three different sections are visible: one part with the highway on a bank, the middle part at the same level of the highway and a third section behind a noise barrier (from North to South). When a bicycle path in the vicinity of a major road is diverging from the traffic lanes, $Avg(L_{OLF})_{p_x}$ is showing an immediate drop, showing detailed spatial effects. The biking trips also sampled on two roads parallel to the highway.

4.2 Statistical analysis of the effect of sparse sampling

Mobile measurements are sparsely sampled databases. The potential use of a parameter depends on its sensitivity to errors introduced by the sparse sampling since less sensitive parameters require less measurement trips. Moreover they will result in more reliable indicators for air pollution as well. The statistics (mean, percentile intervals, and outliers) of the standard deviations $sd(L_{OLF})_{p_x}$ and $sd(L_{Aeq})_{p_x}$ over all locations p_x, are shown in Figure 2 as a function of value classes. The mean and upper percentiles of $sd(L_{OLF})_{p_x}$ are lower than the corresponding values of $sd(L_{Aeq})_{p_x}$ indicating indeed that $Avg(L_{OLF})_{p_x}$ is less sensitive to sparse sampling than $Avg(L_{Aeq})_{p_x}$. It is also important to note the strong dependence of $sd(L_{Aeq})_{p_x}$ on the parameter value. This results from the event-like time series of $L_{Aeq,1s}$ in the aggregation points: low levels correspond to cycling routes free of traffic so only the slowly varying background contributes while very high values are caused by roads carrying so much traffic that the sparse sampling again does not result in high variability.

The relation between the standard error on the average and the number of passages is shown in Figure 3. The median over all observation points, p_x, of the standard error of $Avg(L_{OLF})_{p_x}$ drops below 1 dB if 4 or more passages are available. Similar results are found for $Avg(L_{OMF})_{p_x}$ and $Avg(L_{HFmLF})_{p_x}$. $Avg(L_{OHF})_{p_x}$, $Avg(L_{OHF})_{p_x}$ and $Avg(L_{Aeq})_{p_x}$ show higher standard errors, with median dropping below 1dB only when more than 10 passages are available.
The standard deviation as a function of the number of passages is also shown in Figure 3. The values are more or less constant for categories with more than 4 passages, which is the hypothesis underlying the analysis of the standard error.

A theoretical evaluation to predict the effects of sparse sampling was performed by Makarewicz (Makarewicz, 2006). His model predicted the error of approximation on simulated data to be 1.3 dB when using 10 samples. In our measurements we found a median value of the standard error

for $Avg(L_{Aeq})_{p_x}$ of 1.5 dB which leads to the conclusion that the theoretical model slightly under predicts the measurement error. The standard error of $Avg(L_{Aeq})_{p_x}$ exceeds 2 dB for a significant part of the distribution.

4.4 Principal component analysis of the mobile noise measurements

A principal component analysis over all measurement locations was performed on the noise parameters. The results are shown in Table 2. In the first component which explains 70% of variance, $Avg(L_{Aeq})_{p_x}$, $Avg(L_{OBF})_{p_x}$, $Avg(L_{OLF})_{p_x}$, $Avg(L_{OMF})_{p_x}$.and $Avg(L_{OHF})_{p_x}$ have a similar strength.. It can be expected that this component is mainly related to traffic intensity since this affects all of the above mentioned parameters in a similar way. The second and the third component explain 14% and 13 % of the variance, respectively. The second component is almost completely defined by $Avg(L_{Aeq} - L_{Amin})_{p_x}$, related to the short term noise dynamics. The third component is mainly explained by $Avg(HFmLF)_{p_x}$, the spectral content of the noise immission. The orthogonality of the spectral content and the noise temporal dynamics is relevant since they describe different traffic conditions. This supports the use of partial spectral evaluations and confirms the added value of $Avg(L_{Aeq} - L_{Amin})_{p_x}$. and $Avg(HFmLF)_{p_x}$ in the mobile noise evaluation.

4 CORRELATION WITH BLACK CARBON MEASUREMENTS

The correlation between the log-transformed averaged local component of black carbon concentration $\mathrm{Log10}(Avg(BC_{local}))_{p_x}$ in the aggregation points and the different noise parameters is calculated restricting the dataset to aggregation points with a minimum of five passages (Table 3). Restricting the aggregation points to a minimum of five passages corresponds with a third quartile of standard error of $Avg(L_{Aeq})_{p_x}$ below 2 dB and a third quartile of the standard error of $Avg(L_{OLF})_{p_x}$below 1.5 dB. The strongest correlation is found for $Avg(OLF)_{p_x}$, $Avg(OMF)_{p_x}$, both for the Pearson and Spearman correlation. The correlation of $Avg(L_{Aeq})_{p_x}$. is slightly lower than the correlation of these partial spectral evaluations. The difference is not as prominent as theoretically predicted in Section 2 because traffic intensity is not taken into account in Section 2 and it was found that this factor explains a large amount of the variance in the data. More importantly, the correlation of $Avg(L_{Aeq} - L_{Amin})_{p_x}$. and $Avg(HFmLF)_{p_x}$ with $\mathrm{Log10}(Avg(BC_{local}))_{p_x}$ is low or negative.

In Figure 4 the relation of $10.\mathrm{Log10}(Avg(BC_{local}))_{p_x}$ is plotted versus $Avg(L_{Aeq})_{p_x}$, $Avg(OLF)_{p_x}$, $Avg(L_{Aeq} - L_{Amin})_{p_x}$ and $Avg(HFmLF)_{p_x}$ for the aggragation points with at least 5 passages. The stronger correlation of BC with $Avg(OLF)_{p_x}$ compared to $Avg(L_{Aeq})_{p_x}$ is clearly visible. $Avg(HFmLF)_{p_x}$ shows a non linear relationship with the black carbon exposure.

The overall correlation of the noise parameters with the Black Carbon is good, but not as strong as expected on the basis of theoretical considerations on emission. This is caused by the strong disturbances of the Black Carbon exposure by local dispersion parameters such as street canyon effects. Modeling air pollution based on noise exposure will therefore have to include local dispersion properties of air pollution to result in a useful model.

5 DISCUSSION AND GUIDELINES FOR MOBILE NOISE MEASUREMENTS

Based on a one year mobile measurement campaign for noise and black carbon, insight was gained on (1) the use of sparse measurement for traffic noise exposure mapping purposes; (2) the use of noise as a proxy for black carbon exposure assessment.

The standard error on L_{Aeq} is comparable to earlier theoretical work. For this typical European city and suburb the variability in the standard error on the sparse measurement over locations is important yet not disastrous. With 10 observations of about 10 seconds – the duration of cycling the 50m measurement grid cell – for example, the standard error on the L_{Aeq} is below 1.5 dBA for half of the locations while it is below 2.5 dBA for 95% of the locations. The measurement error depends on L_{Aeq} with standard deviations between measurements at a given location peaking between 57.5 and 72.5 dBA. At higher and lower noise levels standard deviations drop and the number of measurements can be reduced with up to a factor of 2 while keeping the measurement error similar. This is also in line with earlier findings.

In view of the use of noise as a proxy for assessing exposure to black carbon, it was theoretically expected that the low frequency part of the noise, L_{OLF} would be of importance because it has a higher theoretical correlation with air pollution emission. This component shows some interesting characteristics. Investigating the effect of the standard deviation as a function of the number of passages shows a median standard deviation of the the L_{OLF} between 2.5 and 3.5 over the full range of passages, and a median standard error of 4 to 5 dB for the L_{Aeq} evaluation. The low frequencies are more stable than the L_{Aeq} evaluation and have therefore a stronger potential to result in stable models for black carbon exposure. A similar effect is visible for the standard error. The median standard error of L_{OLF} reaches 1.5 dB starting from 5 passages, a level that is not even met with 10 passages for the L_{Aeq}. The spatial difference between the L_{Aeq} and L_{OLF} is also showing some interesting features related to the local traffic noise emission. Near crossings, traffic lights and roads with dense and congested traffic the L_{OLF} results in relatively higher levels than L_{Aeq}. This indicates a stronger contribution of the engine noise in the overall noise level at these areas and potentially higher emission of air pollutants.

Additional noise indicators that could be useful proxies for black carbon were investigated. Principle component analysis shows that the L_{Aeq} and all spectral indicators match an underlying factor explaining most of the variance, probably straight forward traffic intensity. As expected on the basis of theoretical emissions, L_{OLF} correlates best with BC exposure measurements amongst the single indicators in this factor. A second principle component relates to the difference between one second L_{Aeq} and minimum value. This could be an indicator of continuous traffic flow or larger distance between the cyclist and the motorized road traffic. The third component relates to the spectral content, the amount of high frequencies compared to low frequencies. Although their correlation with BC concentration is weaker than the correlation with the first component, these two additional orthogonal indicators could prove useful in modeling BC exposure on the basis of noise monitoring.

When there is an interest in analyzing traffic noise for example for predicting air pollution it is therefore recommended to measure at least one-third octave band spectra and repeat measurements at least every second but preferably ten times per second. A statistical evaluation (min/max) within the sampled second might be an alternative to the sub second time sampling.

6 CONCLUSIONS

Mobile noise measurements (bicycle, on foot) have the potential to improve the noise mapping by introducing local noise characteristics currently not including in the noise mapping. In this paper it was shown on the basis of an extensive measurement campaign that accurate results can be obtained with as few as ten to twenty passages at every grid location.
Spectral and temporal information can give insight in traffic dynamics and related perception of the sonic environment. These traffic dynamics might be even more important when it comes to predicting exposure to air pollution caused by local traffic sources. To ensure the extended use of the mobile noise measurements, a good temporal resolution and a detailed spectral evaluation in third octave bands is recommended.

7 REFERENCES

Can, A. and D. Botteldooren (2011). "Towards Traffic Situation Noise Emission Models." Acta Acustica United with Acustica **97**(5): 900-903.

Can, A., L. Dekoninck, et al. (2011). "Noise measurements as proxies for traffic parameters in monitoring networks." Science of the Total Environment **410**: 198-204.

Can, A., L. Leclercq, et al. (2010). "Traffic noise spectrum analysis: Dynamic modeling vs. experimental observations." Applied Acoustics **71**(8): 764-770.

De Coensel, B., D. Botteldooren, et al. (2007). "Microsimulation based corrections on the road traffic noise emission near intersections." Acta Acustica United with Acustica **93**(2): 241-252.

Eisenman, S. B., E. Miluzzo, et al. (2009). "BikeNet: A Mobile Sensing System for Cyclist Experience Mapping." Acm Transactions on Sensor Networks **6**(1).

Foraster, M., A. Deltell, et al. (2011). "Local determinants of road traffic noise levels versus determinants of air pollution levels in a Mediterranean city." Environmental Research **111**(1): 177-183.

Kanjo, E. (2010). "NoiseSPY: A Real-Time Mobile Phone Platform for Urban Noise Monitoring and Mapping." Mobile Networks & Applications **15**(4): 562-574.

Maisonneuve, N., M. Stevens, et al. (2009). "NoiseTube: Measuring and mapping noise pollution with mobile phones." Information Technologies in Environmental Engineering: 215-228.

Makarewicz, R. and R. Golebiewski (2006). "Estimation of the A-weighted long term average sound level." Acta Acustica United with Acustica **92**(4): 574-577.

Salomons, E., D. van Maercke, et al. (2011). "The Harmonoise Sound Propagation Model." Acta Acustica United with Acustica **97**(1): 62-74.

Smit, R., R. Smokers, et al. (2007). "A new modelling approach for road traffic emissions: VERSIT+." Transportation Research Part D-Transport and Environment **12**(6): 414-422.

Table 1 – Correlation table for the spectral noise parameters versus air pollution parameters .

	$L_{Aeq,1s}$	$L_{OBFeq,1s}$	$L_{OLFeq,1s}$	$L_{OMFeq,1s}$	$L_{OHFeq,1s}$	$L_{HFmLF,1s}$
Log10(CO_2)	0.358	0.913	0.665	0.522	0.305	-0.195
Log10(NO_x)	0.633	0.890	0.857	0.764	0.580	0.020
Log10(PM_{10})	-0.073	0.721	0.313	0.091	-0.120	-0.476

Table 2 - Principal Component Analysis of the aggregation points along the network.

Importance of components:				
	Comp.1	Comp.2	Comp.3	Comp.4
Standard deviation	2.219	0.998	0.942	0.339
Proportion of Variance	0.704	0.142	0.126	0.016
Cumulative Proportion	0.704	0.846	0.973	0.989
Loadings				
$Avg(L_{Aeq})_{p_x}$.	0.430	-0.219		-0.121
$Avg(L_{Aeq} - L_{Amin})_{p_x}$.	-0.118	-0.964		0.171
$Avg(OBF)_{p_x}$.	0.398		-0.392	0.807
$Avg(OLF)_{p_x}$.	0.424		-0.323	-0.257
$Avg(OMF)_{p_x}$.	0.438			-0.410
$Avg(OHF)_{p_x}$.	0.443		0.165	
$Avg(HFmLF)_{p_x}$.	0.272		0.838	0.256

Table 3 - Pearson and Spearman correlation between $Log10(Avg(HFmLF))_{p_x}$. and the different noise parameters for aggregation points with a minimum of five passages.

	Minimum 5 passages	
Noise Parameter	Pearson	Spearman
$Avg(L_{Aeq})_{p_x}$.	0.593	0.601
$Avg(L_{Aeq} - L_{Amin})_{p_x}$	-0.246	-0.296
$Avg(OBF)_{p_x}$.	0.614	0.624
$Avg(OLF)_{p_x}$.	0.652	0.664
$Avg(OMF)_{p_x}$.	0.656	0.667
$Avg(OHF)_{p_x}$.	0.590	0.598
$Avg(HFmLF)_{p_x}$.	0.320	0.341

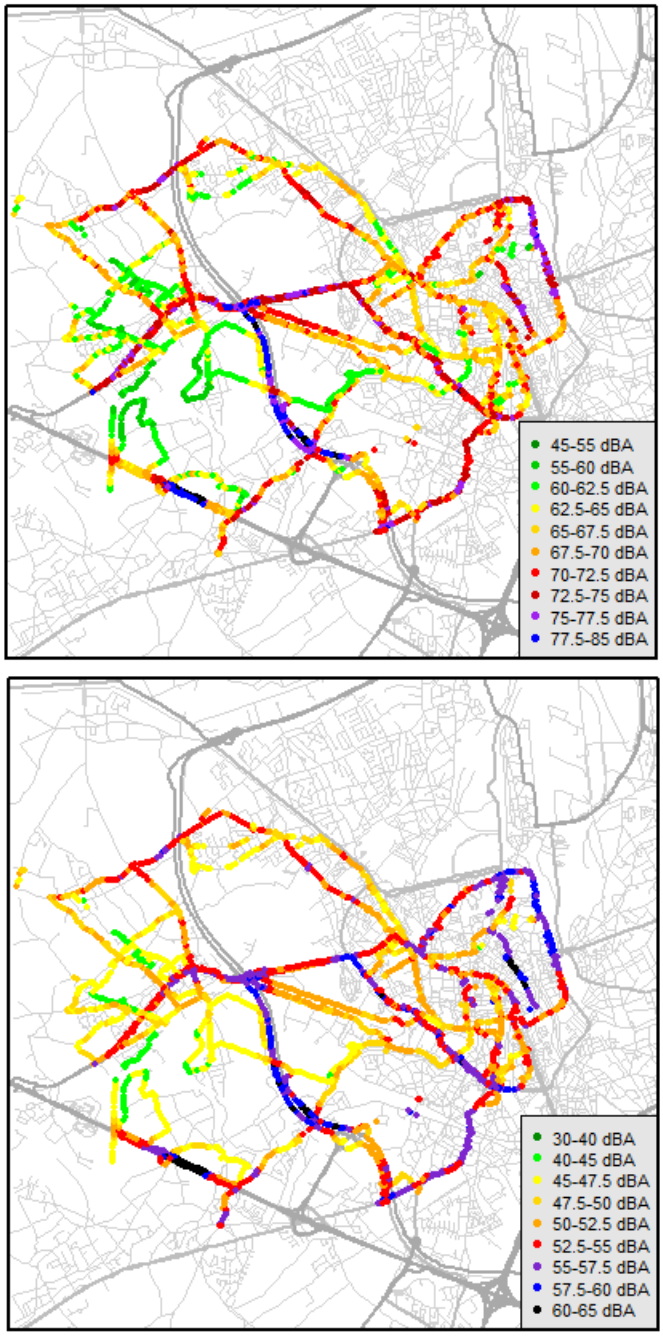

Figure 1 $Avg(L_{Aeq})_{p_x}$ *(upper) and* $Avg(L_{OLF})_{p_x}$ *(lower) in the aggregation points along the network.*

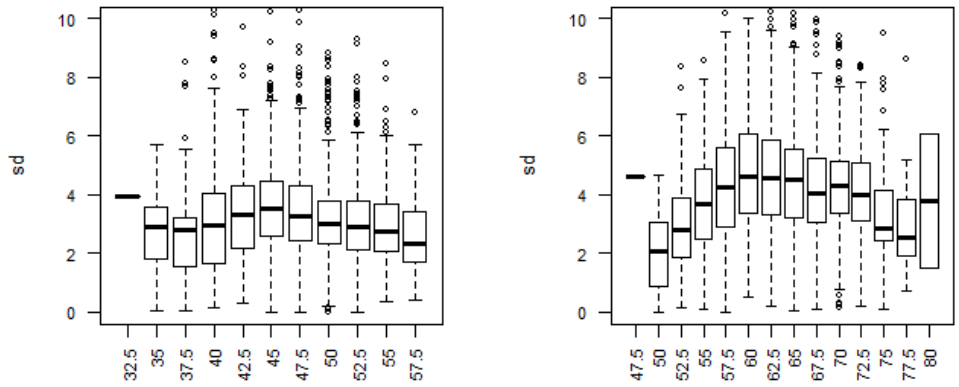

Figure 2 - Statistics (median, percentile intervals, outliers) over locations p_x of the standard deviation $sd(L_{OLF})_{p_x}$(left) and $sd(L_{Aeq})_{p_x}$ (right) as a function of 2.5 dB value classes of $Avg(L_{Aeq})_{p_x}$.

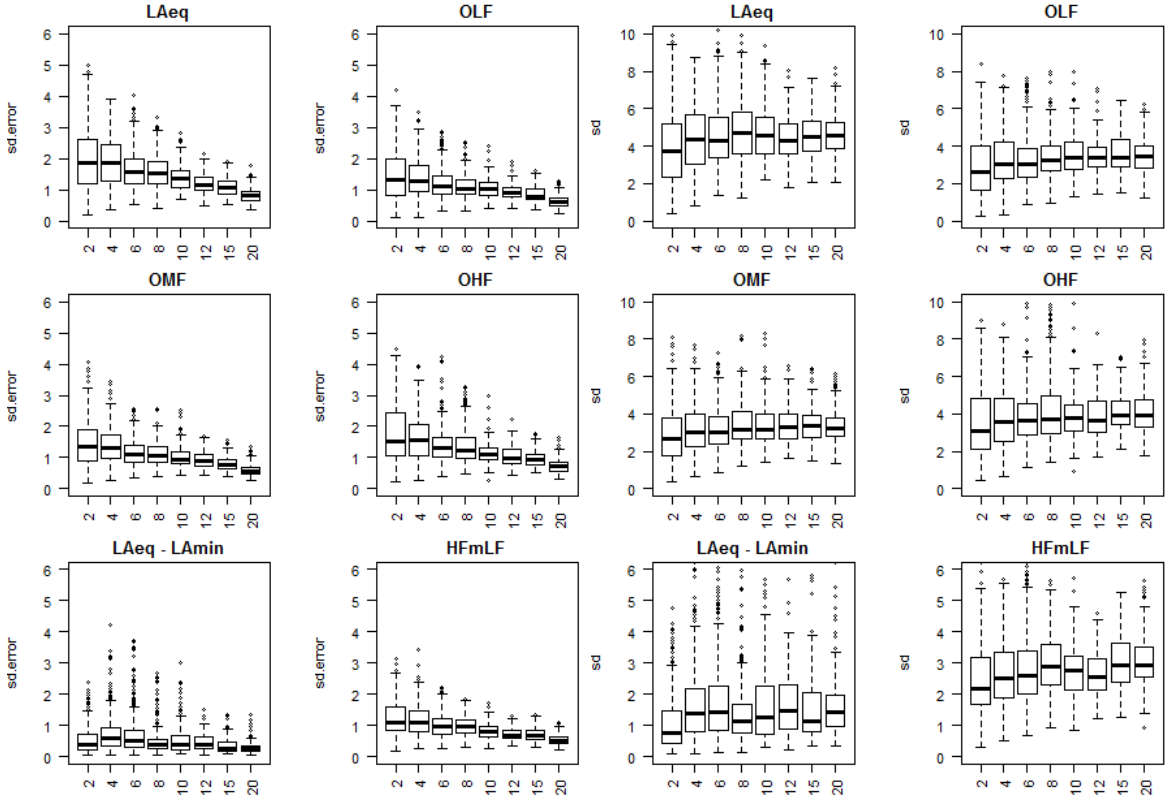

Figure 3 - Statistics (median, percentile intervals, outliers) over locations p_x of the standard error (left) and standard deviation (right) as a function of the number of passages.

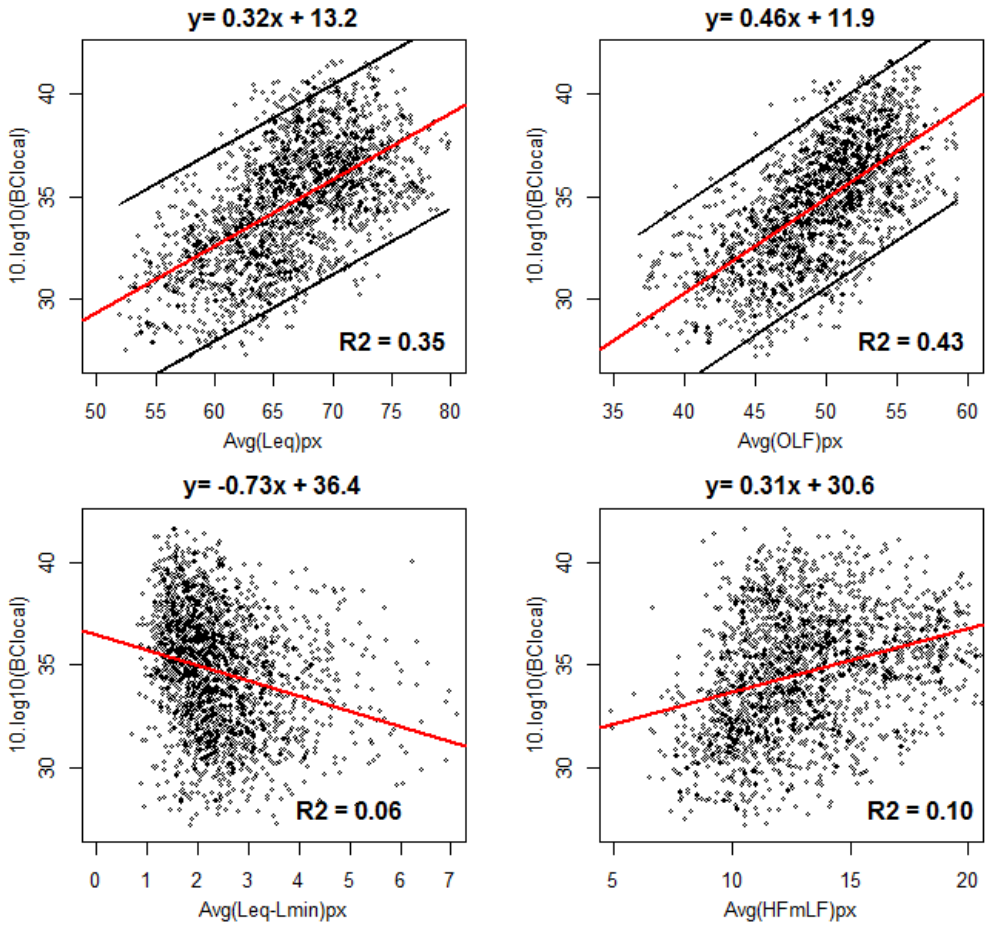

Figure 4 - Linear model of Black Carbon ($10.Log10(Avg(BC_{local}))_{p_x}$*) with* $Avg(L_{Aeq})_{p_x}$*.,* $Avg(OLF)_{p_x}$*.* $Avg(L_{Aeq} - L_{Amin})_{p_x}$ *and* $Avg(HFmLF)_{p_x}$*. Prediction intervals 95%) are included for* $Avg(L_{Aeq})_{p_x}$*. and* $Avg(OLF)_{p_x}$*.*